Dehydrogenation and aromatization of methane in the absence of oxygen on Mo/HZSM-5 catalysts before and after NH_4OH extraction

Yide Xu [1], Wei Liu, She-Tin Wong, Linsheng Wang and Xiexian Guo

State Key Laboratory of Catalysis, Dalian Institute of Chemical Physics, Chinese Academy of Sciences, PO Box 110, Dalian 116023, PR China

Received 30 January 1996; accepted 28 May 1996

Mo/HZSM-5 catalysts show good catalytic reactivity in the absence of oxygen for the dehydrogenation and aromatization of methane at 973 K. The active Mo species were investigated by combining catalytic studies on Mo/HZSM-5 catalysts before and after NH_4OH extraction with XRD, BET, NH_3-TPD and TPR analysis. The XRD patterns show that Mo species are well dispersed on the zeolite surface. The specific surface areas decrease with increasing Mo loading but they can be restored to a large extent by NH_4OH extraction. NH_3-TPD results suggest that the Mo species prefer to deposit on the strong acid sites of HZSM-5 zeolite. TPR profiles show that there is a kind of Mo species which is easily reduced. No TPR peaks could be obviously observed if the Mo/HZSM-5 catalysts were extracted by NH_4OH solution. The results of NH_4OH extraction experiment and other relevant characterization studies suggest that there are several kinds of Mo species deposited on the surface. By referring to the Mo species on Al_2O_3 supported MoO_3 samples, we propose that the dissolvable Mo species in NH_4OH solution are MoO_3 crystallites and their aggregates in octahedral coordination, while the unsoluble Mo species mainly are $Al_2(MoO_4)_3$ and MoO_4^{2-} in tetrahedrally coordinated form. The catalytic performance of Mo/HZSM-5 catalysts before and after NH_4OH extraction illustrates that Mo species in small MoO_3 crystallites with octahedral coordination form are active for methane activation in the absence of oxygen on Mo/HZSM-5 catalysts, while Mo species in tetrahedrally coordinated form is less active for the reaction.

Keywords: Mo/HZSM-5; Mo species; MoO_3 crystallites; $Al_2(MoO_4)_3$ crystallites; methane activation; NH_4OH extraction

1. Introduction

ZSM-5 zeolite and its modification have received considerable interest in the field of heterogeneous catalysis for years because of their superb coking resistance [1] and unique acid and shape selective properties [2]. Mo/HZSM-5 catalysts are usually considered as potential hydrotreating catalysts for industrial application [3,4].

Recently, we were the first to report that methane can be activated in the absence of O_2 via dehydrogenation and aromatization processes on Mo/HZSM-5 catalysts for the formation of benzene and toluene [5]. Ethylene is the initial product. The outstanding catalytic behavior of Mo/HZSM-5 catalyst has been attributed to several factors such as the location and state of Mo species and the acidity and channel structure of HZSM-5 zeolite [6–12]. In our previous study on Mo/HZSM-5 catalysts, the existence of two kinds of Mo species, MoO_3 and $Al_2(MoO_4)_3$ crystallites, have been suggested [10]. In comparison with alumina supported metal oxide catalysts, ZSM-5 zeolite supported metal oxide catalysts are much less known and are under investigation by many research groups. Fortunately, oxides such as Al_2O_3 and SiO_2 etc. supported MoO_3 catalysts have been well studied [13–17]. Despite the many works that have been repeatedly reported in the literature, disagreement on the nature of Mo species still exists. Anyway, most of these studies claim that several kinds of Mo species can be detected. When Mo loading is lower than monolayer coverage, there are Mo species in both tetrahedrally and octahedrally coordinated forms. When Mo loading is higher than monolayer coverage, MoO_3 crystallites with Mo cation octahedrally coordinated to oxygen and $Al_2(MoO_4)_3$ crystallites with Mo cation tetrahedrally coordinated to oxygen can be detected. It is well known that MoO_3 crystallites in octahedrally coordinated form can be easily dissolved while $Al_2(MoO_4)_3$ and MoO_4^{2-} species in tetrahedrally coordinated form cannot be dissolved by NH_4OH solution. Moreover, MoO_3 crystallites are easily reduced with H_2 while $Al_2(MoO_4)_3$ and MoO_4^{2-} are almost irreducible under conventional conditions (if the reduction temperature is lower than 1000 K). Although the surface composition of ZSM-5 zeolite is different from that of Al_2O_3 oxide, for OH groups, Si–OH might act like Al–OH. Therefore, the techniques of NH_4OH extraction and temperature programmed reduction (TPR) may also be useful for distinguishing Mo species on Mo/HZSM-5 catalysts.

In this paper, methane aromatization in the absence of oxygen on Mo/HZSM-5 catalysts before and after NH_4OH extraction was investigated by combining catalytic studies with XRD, BET, NH_3-temperature programmed desorption (NH_3-TPD) and TPR techniques in order to shed light on the nature of active Mo species

---

[1] To whom correspondence should be addressed.

and the interaction between Mo species and HZSM-5 zeolite.

2. Experimental

2.1. Catalyst preparation and NH_4OH extraction

HZSM-5 zeolite with a SiO_2/Al_2O_3 mole ratio of 50 was supplied by Nankai University and was used without further treatment. Catalysts with Mo loading ranging from 1 to 15% were prepared by impregnating HZSM-5 with aqueous solutions of ammonium heptamolybdate. The samples were then dried at 383 K overnight and calcined in air at 773 K for 6 h. The calcined samples were tableted, crushed and sieved to 40–60 mesh before use.

The calcined samples (about 4 g of each sample) were extracted with 400 ml of dilute NH_4OH solution (5 vol% of NH_3) for 72 h. The amount of soluble Mo species was determined by ultraviolet and visible spectroscopy [18]. The NH_4OH-extracted samples were then dried at 383 K and calcined at 773 K for 6 h. The Mo/HZSM-5 catalysts before and after NH_4OH extraction are referred to hereafter as xMo/HZ and xMo/HZ-N, respectively. x and N denote Mo content and the catalyst after NH_4OH extraction, respectively.

2.2. Characterization of Mo/HZSM-5 zeolite catalysts

X-ray powder diffraction patterns were obtained on a Rigaku diffractometer using Cu-K_α radiation at room temperature. Powder diffractograms of samples were recorded over a range of 2θ values from 5–50° under the conditions of 40 kV and 100 mA at a scanning rate of 8 deg/min. All the XRD patterns recorded can be processed with a computer system attached to the instrument.

Specific surface areas and average pore diameters of the samples were obtained by the BET method at liquid nitrogen temperature with a Micromeritics ASAP-2000 instrument and data were processed and analyzed by an IBM computer.

The NH_3-TPD experiment was performed on a conventional TPD apparatus using a thermal conductivity detector. About 0.14 g of sample was placed in a quartz reactor and heated under He at 873 K for 40 min, then cooled to 423 K and saturated with ammonia. TPD was carried out from 423 to 873 K at a heating rate of 25 K/min using helium as the carrier gas.

TPR was carried out on a conventional apparatus like NH_3-TPD. About 0.1 g of sample was placed in a quartz reactor and flushed with N_2, then heated in air at 973 K for 40 min and finally cooled to room temperature under N_2. The sample was then reduced under a H_2–N_2 (10 vol% of H_2) stream at a flow rate of 35 ml/min and a heating rate of 8 K/min from room temperature to 1109 K, followed by a heating rate of 5 K/min to 1173 K.

2.3. CH_4 dehydrogenation and aromatization

Catalytic tests were performed with a fixed bed continuous-flow quartz reactor with 8 mm i.d. as mentioned in our previous papers [6,7,10]. Normally, the catalyst charge was 0.2 g. It was heated under an air stream (15 ml/min) to 973 K and maintained at 973 K for 40 min. After the pretreatment stage, methane was introduced into the reactor through a Brooks mass flow controller at a space velocity of 1500 ml CH_4 per gram of catalyst per hour. The pressure of the reactor system was 115 kPa and the reaction temperature was 973 K in a standard test. The tail gas was sampled periodically after 40 min running and analyzed by a Shimadzu GC-9AM gas chromatograph. The conversion of methane (C_{CH_4}), the product yields of aromatics (mainly benzene), ethylene and ethane (Y_{ar}, $Y_{C_2H_4}$, and $Y_{C_2H_6}$) and the selectivity to aromatics (S_{ar}) and hydrocarbons (S_{HC}) were calculated on the basis of carbon number balance. Methane was 99.95% pure. Analysis of the air and helium used in the experiment showed the absence of any H_2 and hydrocarbons.

3. Results and discussion

3.1. NH_4OH extraction of Mo/HZSM-5 catalysts and the states of Mo species

The results of NH_4OH extraction show that there are two kinds of Mo species on Mo/HZSM-5 catalysts. One is soluble (NH_4OH-extracted Mo) and the other (residual Mo) cannot be dissolved by NH_4OH solution. Fig. 1 shows that the amount of NH_4OH-extracted Mo

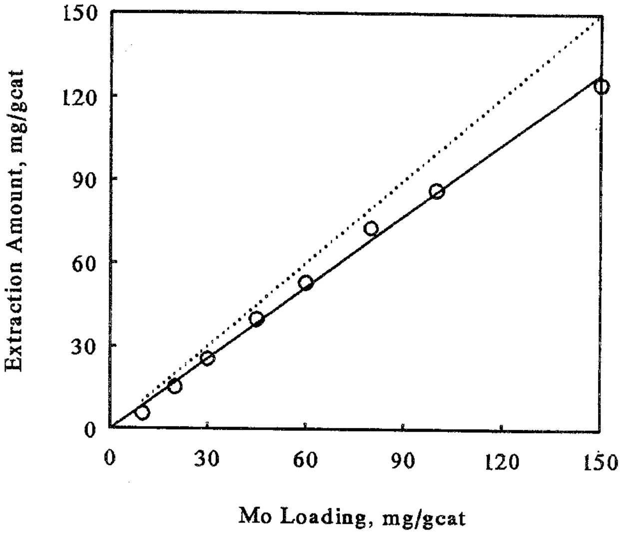

Fig. 1. The linear relationship between the amount of NH_4OH extracted Mo and Mo loading. (○) and solid line: experimental; dotted line: if all Mo species were extracted by NH_4OH.

on Mo/HZSM-5 catalysts increases linearly with Mo loading. Meanwhile, the dependence of the amount of residual Mo on original Mo loading seems to be more complicated (see table 1). If the Mo loading is less than 3.0%, the amount of residual Mo is almost the same (about 0.5%) within experimental error, while if Mo loading is higher than 3.0%, the amount of residual Mo increases with Mo loading. The non-linear dependence of the amount of residual Mo on Mo loading implies that there are several kinds of Mo species at different Mo loading on the zeolite surface.

The structure of Mo species on oxide support such as Al_2O_3 has been widely studied [13–17,19–22]. Monolayer structures I and II with Mo cation in tetrahedral and octahedral coordination, respectively, have been suggested. The tetrahedrally coordinated Mo species in the monolayer state are presumably formed first in the initial stages of impregnation through reaction between OH groups on Al_2O_3 surface and MoO_4^{2-} or $Mo_7O_{24}^{6-}$ anionic species in the impregnating solution according to the reaction as follows:

$$8Al_sOH + Mo_7O_{24}^{6-} \rightarrow 4(Al_s)_2MoO_4 + 3MoO_4^{2-} + 4H_2O$$

in which *s* denotes a surface Al species. Arnoldy [21] also proposed a structure for the Mo species as shown in I.

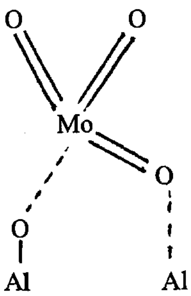

I

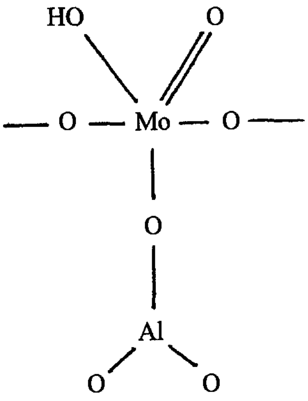

II

In structure I, each Mo cation has three Mo=O bonds which are not equivalent, and a bridging oxygen which is bound strongly to an Al cation exposed on the surface. The interaction between the Mo cation and the support is indicated by dotted lines. In this case, one Mo cation interacts with two Al cations, one is via a bridging oxygen and the other via an interaction with a coordinatively unsaturated Al cation. This will produce a tetrahedrally coordinated Mo. The octahedrally coordinated Mo species can be formed as expressed in structure II [19]. In this case, only one Al cation is involved. As far as the surface OH groups are concerned, Si–OH might act like Al–OH. We may, therefore, assume that Mo species deposited on HZSM-5 zeolite are similar to those deposited on Al_2O_3 support. Therefore, in the early stages of impregnation, this type of octahedrally coordinated Mo species exists in a monolayer state. We may suppose that the interaction between an octahedrally coordinated Mo species and the support is not as strong as between a tetrahedrally coordinated Mo species and the support. Anyway, the tetrahedrally coordinated Mo species cannot be dissolved and the octahedrally coordinated Mo species in their monolayer states might be difficult to be dissolved by NH_4OH solution. To determine the ratio between the tetrahedrally and octahedrally coordinated Mo species on the surface at saturation monolayer coverage is rather difficult since their formation may depend on many factors such as the pH value of impregnating solution, the mole ratio of SiO_2/Al_2O_3 of the zeolite used, the Mo loading, the calcination temperature and so on [13–17].

If Mo loading is higher than the monolayer coverage of the support, MoO_3 crystallites which are in octahedral coordination form may be easily formed on the zeolite surface [23] and can be dissolved by NH_4OH solution. On the other hand, $Al_2(MoO_4)_3$ crystallites can also form. The formation of $Al_2(MoO_4)_3$ crystallites and MoO_4^{2-} species in which the Mo cations are tetrahedrally coordinated can be attributed to several factors: the strong interaction between Mo species and non-framework Al cations (which always exist on zeolites), the migration of Mo species into the zeolite channels and the extraction of Al cations from the framework of HZSM-5 zeolite by Mo species. The last two factors have been well recognized [23,24]. Therefore, in the case of Mo loading higher than the monolayer coverage during the impreg-

Table 1
Mo content of Mo/HZSM-5 catalysts before and after NH_4OH extraction

Sample	Total Mo (mg/g cat)	NH_4OH extract. (mg/g cat)	Residual Mo (mg/g cat)	Ratio of octa. Mo and tetra. Mo
1Mo/HZ	10	5.5	4.5	1.2
2Mo/HZ	20	15.2	4.8	3.2
3Mo/HZ	30	25.4	4.6	5.5
4.5Mo/HZ	45	39.9	5.1	7.8
6Mo/HZ	60	53.1	6.9	7.7
8Mo/HZ	80	72.8	7.2	10.1
10Mo/HZ	100	86.5	13.5	6.4
15Mo/HZ	150	125.0	25.0	5.0

nation of the zeolite with aqueous solution of ammonium heptamolybdate, the formation of tetrahedrally coordinated Mo increases with Mo loading.

The results of our NH_4OH extraction experiment show that when Mo loading ranges from 1 to 3%, the amount of NH_4OH-extracted Mo increases with increasing Mo loading but the amount of residual Mo on the zeolite remains almost unchanged. This suggests that the monolayer coverage of the zeolite used in this work occurred at about 0.5% of Mo loading. The amounts of NH_4OH-extracted Mo and residual Mo increase with Mo loading when the Mo loading ranges from 3 to 8%. On the average, about 90% of the Mo species on the zeolites are octahedrally coordinated and are extractable by NH_4OH solution at this range of Mo loadings. At the same time, this also implies that tetrahedrally coordinated $Al_2(MoO_4)_3$, which cannot be dissolved by NH_4OH solution, is formed simultaneously. When Mo loading is higher than 8%, the formation of $Al_2(MoO_4)_3$ aggregates is even more favored since the ratio of octahedrally coordinated and tetrahedrally coordinated Mo species decreases with Mo loading.

The results of XRD analysis on Mo/HZSM-5 catalysts and mechanical mixtures of MoO_3 and HZSM-5 with different Mo loadings are listed in table 2. For comparison, table 2 also includes the results of pure MoO_3. For the mechanical mixture with Mo content as low as 1%, the MoO_3 phase is detectable as we can see from table 2. No corresponding Mo species could be observed in the XRD patterns of Mo/HZSM-5 catalysts which were calcined at 773 K for 6 h. Therefore, Mo species on Mo/HZSM-5 catalysts prepared by impregnation are well dispersed on the zeolite surface and the crystallites of MoO_3 and $Al_2(MoO_4)_3$ are smaller than 4 nm and cannot be detected by XRD technique.

Fig. 2 shows the BET surface areas of the samples before and after NH_4OH extraction. Before NH_4OH extraction, the BET surface areas of the Mo/HZSM-5 catalysts decrease with Mo loading. For the Mo/HZSM-5 catalyst with lower Mo loading, the Mo species are well dispersed on the external surface of HZSM-5. Therefore, it is reasonable to suppose that, at the initial stages of impregnation, Mo species are most likely to deposit on the external surfaces of the zeolite. When Mo loading is higher, Mo species will partly aggregate at the mouth of the channels and partly migrate into the channels. Cations in polyvalent states, like Mo cations, generally show a tendency to move into channels where they can be usually coordinated to a greater number of oxygen ions [25]. The aggregation of Mo species at the mouth of the channels will lead to the blockage of the channels and thus reduce the measured BET surface area of the catalyst. This explanation also agrees with our FT-IR observation [10]. We detected a band at 850 cm^{-1} after the sample was calcined at 573 K which may be attributed to MoO_3 crystallites on the external surface. This band disappeared after the sample was calcined at 773 K, due to the decrease in concentration of MoO_3 via migration of Mo species.

The BET surface areas are restored to a large extent after the Mo/HZSM-5 catalysts were treated with NH_4OH solution. This supports our speculation that MoO_3 crystallites in the octahedral coordination form which blocked the channels of the zeolite have been

Table 2
2θ and *d*-spacing from XRD characteristic peaks of Mo species and HZSM-5

Sample	Mechanical mixture			Impregnated Mo/HZSM-5		
	2θ	*d*-spacing (nm)	relative intensity	2θ	*d*-spacing (nm)	relative intensity
MoO_3	39.06	0.230	68			
1Mo	39.02	0.231	15	–	–	
2Mo	38.98	0.231	23	–	–	
3Mo	38.98	0.231	17	–	–	
4.5Mo	39.08	0.230	57	–	–	
6Mo	39.06	0.230	62	–	–	
8Mo	39.06	0.230	65	–	–	
10Mo	39.18	0.230	54	–	–	
15Mo	39.16	0.230	67	–	–	
HZSM-5	23.16	0.384				
1Mo	23.26	0.382	1216	23.28	0.382	903
2Mo	23.28	0.382	1207	23.42	0.380	881
3Mo	23.30	0.381	1203	23.22	0.383	831
4.5Mo	23.36	0.380	1105	23.40	0.380	685
6Mo	23.36	0.380	1072	23.30	0.381	830
8Mo	23.34	0.381	992	23.36	0.380	621
10Mo	23.48	0.379	794	23.30	0.385	801
15Mo	23.46	0.379	780	23.44	0.379	725

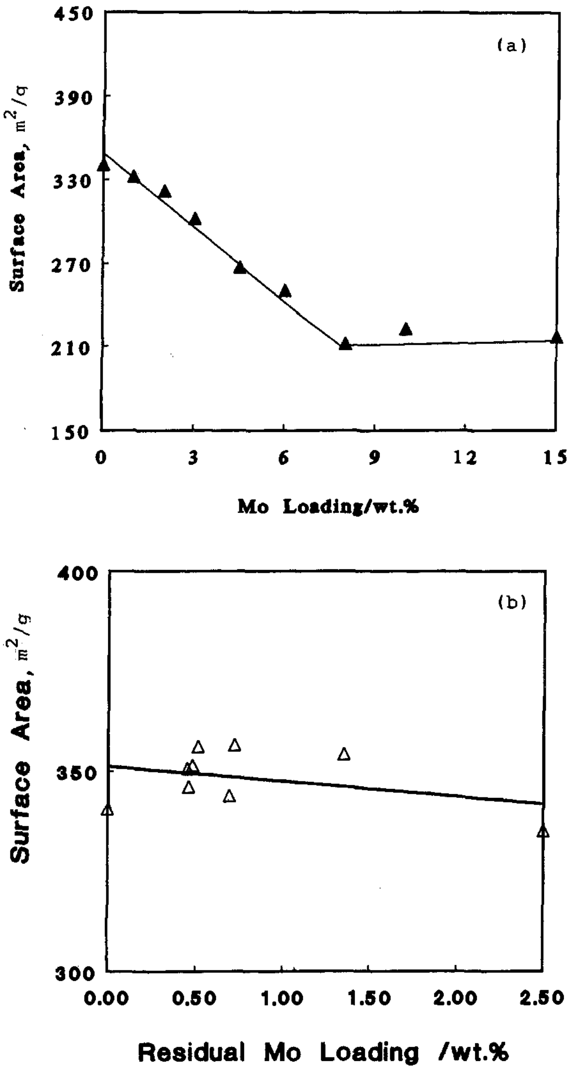

Fig. 2. The changes of BET surface area with Mo loading. (a) Before (▲) NH_4OH extraction; (b) after (△) NH_4OH extraction.

removed by NH_4OH extraction, and the remaining Mo species in the form of tetrahedrally coordinated MoO_4^{2-} are well dispersed in the channels and/or on the external surface.

3.2. Acidity and reducibility of Mo/HZSM-5 before and after NH_4OH extraction

Figs. 3 and 4 show the NH_3-TPD profiles of the samples before and after NH_4OH extraction. Two peaks can be observed on the profiles of HZSM-5 zeolite. One is at 543 K (named as peak L) resulting from the desorption of NH_3 from weak acid sites and the other at 763 K (named as peak H) from strong acid sites. The NH_3-TPD results are in good agreement with those reported by Topsøe [26] and Yang [27]. With increasing Mo loading, the area of peak H decreases but that of peak L shows little change. When Mo loading is 10%, the strong acid sites are nearly eliminated but some new acid sites of medium strength are generated with peak temperature in the range of about 583–593 K. The area of peak L decreases a little bit and its peak temperature moves towards lower temperature with increasing Mo loading.

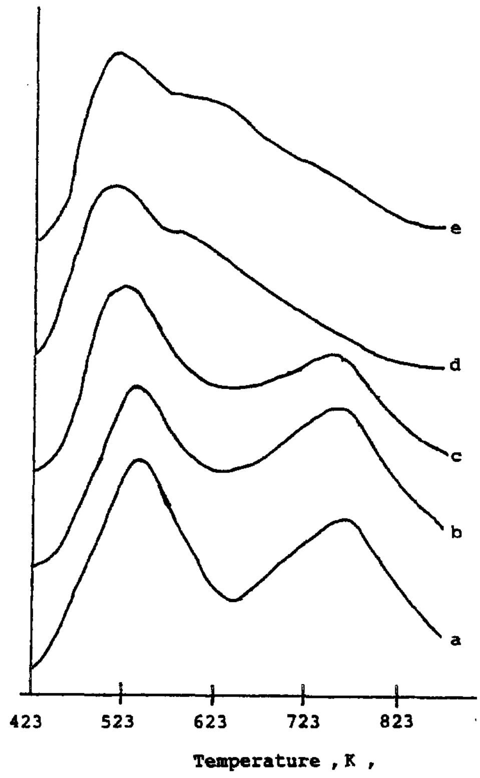

Fig. 3. NH_3-TPD profiles of Mo/HZSM-5 catalysts before NH_4OH extraction. (a) HZSM-5; (b) 1Mo/HZ; (c) 3Mo/HZ; (d) 10Mo/HZ; (e) 15Mo/HZ.

Many authors have suggested that peak L may be attributed to physisorbed NH_3 species and NH_3 adspecies residing on non-exchangeable cationic sites, while peak H results from the desorption of NH_3 adspecies adsorbed on exchangeable protonic sites, i.e. Brønsted type aid sites, which are located at the channel intersections of the zeolites [26–29]. The suppression of strong acidic sites with increasing Mo loading was also reported in ref. [29]. The authors suggested that the introduction of Mo species leads to an interaction between Mo species and the OH groups of the zeolite [23]. Since the Brønsted acid sites are located at the channel intersections of the HZSM-5 zeolite, when Mo loading is high, part of the Mo species must have migrated into the channels and interact with the Brønsted acid sites. These Mo species will consume the Brønsted acid sites. So, when Mo loading is as high as 10%, the strong acidic sites diminish substantially. Meanwhile, acid sites of medium strength appear. This phenomenon has been studied by Davidova et al. [4]. MoO_3 crystallites, which are the main species on silica-rich supports, can generate Lewis acidity associated with Mo coordinatively unsaturated sites (CUS) [30]. A similar result was reported for the introduction of Ga into HZSM-5 zeolite, where Lewis acid sites were developed on the surface [28].

The NH_3-TPD profiles of Mo/HZSM-5 catalysts after NH_4OH extraction show that strong acid sites are restored to some extent, as we can see in fig. 4. This may imply that the interaction between Mo species in octahedrally coordinated form and strong acid sites on the zeolite surface is not very strong, since, as far as the solubility in NH_4OH solution is concerned, MoO_3 crystallites located on the strong acid sites show nearly the same property as in the bulk phase.

Fig. 5 shows the TPR profiles of Mo/HZSM-5 samples before NH_4OH extraction. The TPR profiles recorded for the samples after NH_4OH extraction show that no Mo species could be reduced. This gives us a clue that after NH_4OH extraction, all of the MoO_3 crystallites in octahedrally coordinated form were washed off. It is well known that MoO_4^{2-} species or $Al_2(MoO_4)_3$ crystallites are irreducible if the temperature is lower than 1173 K [31]. The TPR profiles in fig. 5 may mainly reflect the reduction of octahedrally coordinated MoO_3 aggregates. The TPR experiments of Mo/HZSM-5 catalysts before and after NH_4OH extraction show that all the residual Mo species left on the surface after NH_4OH extraction are most probably tetrahedrally coordinated. Despite the difference in Mo loading in the tested Mo/HZSM-5 catalysts, the experimental procedure of NH_4OH extraction adopted in this work is successful in removing all the reducible Mo species on the zeolite surface.

3.3. Dehydrogenation and aromatization of methane on Mo/HZSM-5 catalysts before and after NH_4OH extraction

Figs. 6 and 7 show the results of the catalytic conversion of methane in the absence of oxygen on Mo/

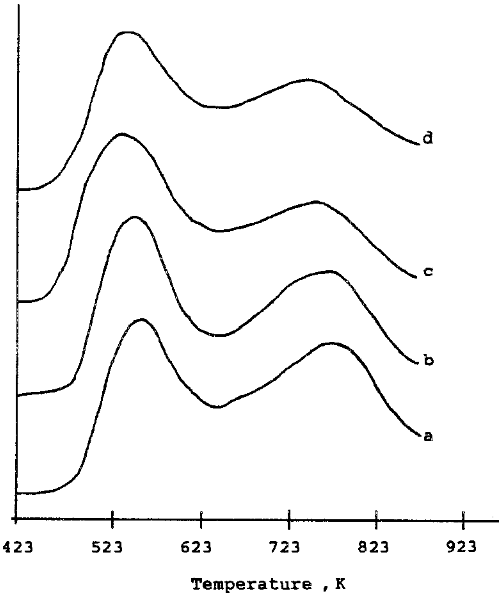

Fig. 4. NH_3-TPD profiles of Mo/HZSM-5 catalysts after NH_4OH extraction. (a) 1Mo/HZ-N; (b) 3Mo/HZ-N; (c) 10Mo/HZ-N; (d) 15Mo/HZ-N.

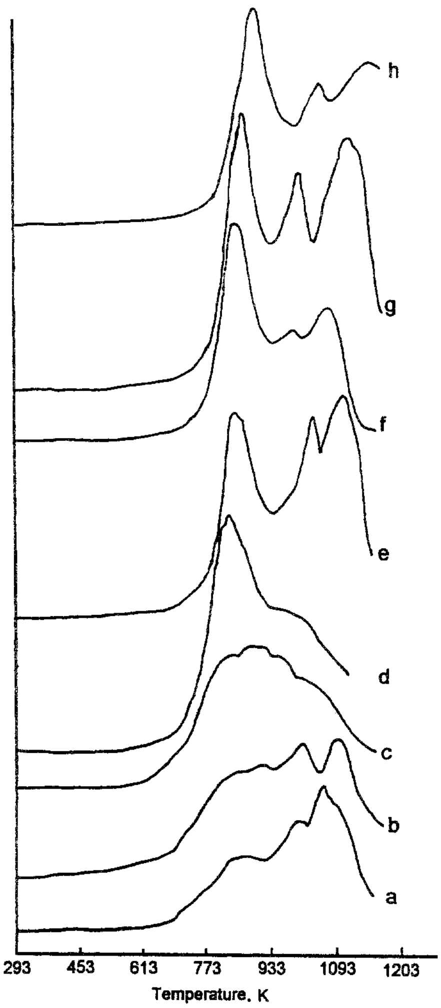

Fig. 5. TPR profiles of Mo/HZSM-5 catalysts before NH_4OH extraction. (a) 1Mo/HZ; (b) 2Mo/HZ; (c) 3Mo/HZ; (d) 4.5Mo/HZ; (e) 6Mo/HZ; (f) 8Mo/HZ; (g) 10Mo/HZ; (h) 15Mo/HZ.

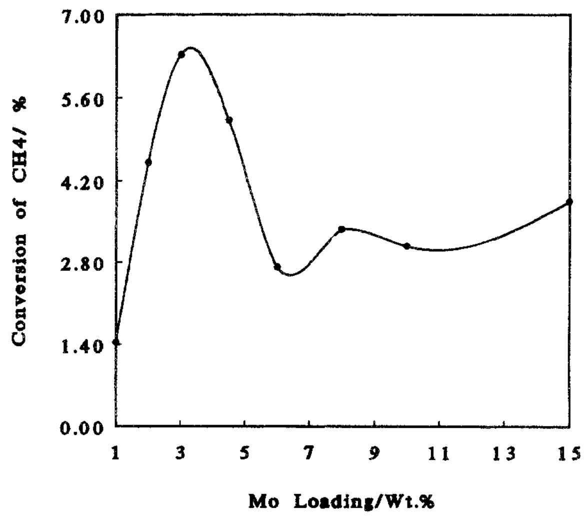

Fig. 6. The CH_4 conversion over Mo/HZSM-5 catalysts before and after NH_4OH extraction.

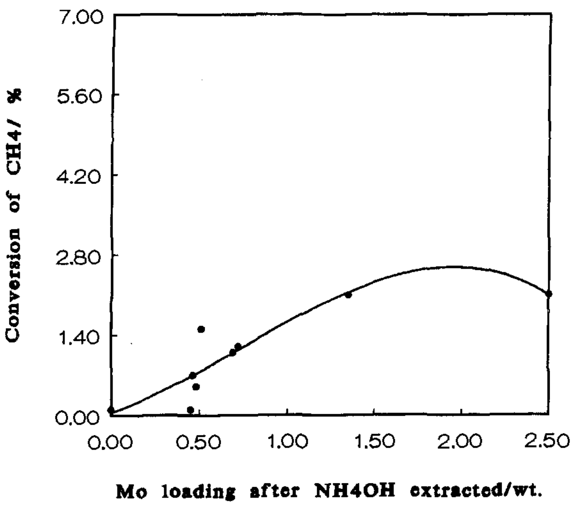

Fig. 7. The CH_4 conversion over Mo/HZSM-5 catalysts after NH_4OH extraction

HZSM-5 catalysts before and after NH_4OH extraction. The results, in more detail, are listed in table 3.

Fig. 6 shows that before NH_4OH extraction, the activity of methane conversion shows a maximum at about 3% Mo loading. Beyond that, it decreases substantially with increasing Mo loading and reaches its lowest level at 6% Mo loading, and then levels off when the Mo loading is higher than 6%. The same trend was obtained in our previous report [6] in which we used NaZSM-5 as a starting material. For the Mo/HZSM-5 catalysts after NH_4OH extraction, the dependence of methane conversion on its residual Mo loading changes a lot. It seems to follow a linear relationship. The dependence of methane conversion on the amount of residual Mo is shown in fig. 7. From table 1, the Mo loading of 15Mo/HZ extracted by NH_4OH is 2.5%, but its activity of methane conversion is much less than that of 2Mo/HZ and/or 3Mo/HZ catalysts. This result appears to suggest that MoO_3 crystallites are active for the dehydrogenation and aromatization of methane in the absence of oxygen while $Al_2(MoO_4)_3$ crystallites are less active.

It was reported that methane can be activated on HZSM-5 zeolite [32,33]. Table 3 shows that the methane conversion is very low over HZSM-5 zeolite. The catalytic activity and selectivity to aromatics are markedly improved on Mo/HZSM-5 catalysts. 3Mo/HZ is the best among the tested catalysts. It is clear that Mo species play an important role in the activation of methane. The activity and selectivity to aromatics decrease obviously on Mo/HZSM-5 catalysts after NH_4OH extraction. Therefore, small MoO_3 crystallites may be the main species active for methane activation while $Al_2(MoO_4)_3$ species are less active for the reaction.

4. Conclusion

Mo species are highly dispersed on HZSM-5 surface. They prefer to deposit on the strong acid sites of HZSM-5 zeolite. Therefore, the concentration of strong acid sites diminished a lot when Mo species are introduced onto HZSM-5.

There are two kinds of Mo species deposited on the surface. One is $Al_2(MoO_4)_3$ in tetrahedral coordination form which cannot be dissolved by NH_4OH solution and the other is MoO_3 in octahedral coordination form which can be dissolved by NH_4OH. If Mo loading is low, both kinds of Mo species will be in monolayer state. With increasing Mo loading, $Al_2(MoO_4)_3$ crystallites in the tetrahedral coordination form and MoO_3 crystallites

Table 3
The conversion of methane and the distribution of product over Mo/HZSM-5 catalysts before and after NH_4OH extraction

Sample	C_{CH_4} (%)	Y_{ar} (%)	$Y_{C_2H_4}$ (%)	$Y_{C_2H_6}$ (%)	S_{HC} (%)	S_{ar} (%)
HZSM-5	0.1	0.0	0.0	0.0	83.2	16.8
1Mo/HZ	1.4	1.2	0.2	0.1	18.0	82.0
2Mo/HZ	4.5	4.2	0.2	0.1	7.1	92.9
3Mo/HZ	6.3	6.0	0.2	0.2	5.2	94.8
4.5Mo/HZ	5.2	4.9	0.2	0.1	6.6	93.4
6Mo/HZ	2.7	2.3	0.2	0.0	13.7	86.3
8Mo/HZ	3.4	3.1	0.2	0.1	8.8	91.2
10MoZ	3.1	2.8	0.2	0.1	10.0	90.0
15Mo/HZ	3.9	3.7	0.1	0.1	5.8	94.2
0.5Mo/HZ-N	0.1	0.0	0.0	0.1	100	0.0
0.5Mo/HZ-N	0.5	0.4	0.1	0.0	19.2	80.8
0.5Mo/HZ-N	0.7	0.5	0.1	0.1	26.9	73.1
0.5Mo/HZ-N	1.5	1.3	0.2	0.1	15.8	84.2
0.7Mo/HZ-N	1.1	0.9	0.1	0.1	18.1	81.9
0.7Mo/HZ-N	1.2	1.0	0.2	0.1	19.0	81.0
1.4Mo/HZ-N	2.1	1.9	0.1	0.1	10.7	89.3
2.5Mo/HZ-N	2.1	1.9	0.1	0.1	11.4	88.6

in the octahedral form are formed and dispersed on the zeolite surface.

The catalytic performances of Mo/HZSM-5 catalysts before and after NH_4OH extraction clearly illustrate that Mo species in the form of MoO_3 crystallites seem to be more active for methane activation in the absence of oxygen than $Al_2(MoO_4)_3$ crystallites.

Acknowledgement

The financial support of the National Natural Science Foundation of China is gratefully acknowledged.

References

[1] S. Yurchak, S.E. Voltz and J.P. Warner, Ind. Eng. Chem. Proc. Res. Devel. 18 (1979) 527.

[2] W.W. Kaeding, C. Chu, L.B. Young, B. Weinstein and S.A. Butter, J. Catal. 67 (1981) 159.

[3] J. Valyon and A. Meszaros-Kirs, in: *Zeolites: Facts, Figure, Future*, Studies in Surface Science and Catalysis, Vol. 49, eds. P.A. Jacobs and R.A. van Santen (Elsevier, Amsterdam, 1989) p. 1015.

[4] N. Davidova, P. Kovacheva and D. Shopov, in: *Proc. 7th Int. Zeolite Conf.*, eds. Y. Murakami, A. Lijima and J.W. Ward (Kodansha, Tokyo, 1986) p. 811.

[5] L. Wang, J. Huang, L. Tao, Y. Xu, M. Xie and G. Xu, Catal. Lett. 21 (1993) 35.

[6] Y. Xu, S. Liu, L. Wang, M. Xie and X. Guo, Catal. Lett. 30 (1995) 135.

[7] L. Wang, Y. Xu, M. Xie, S. Liu and L. Tao, Stud. Surf. Sci. Catal. 94 (1995) 495.

[8] F. Solymosi, A. Erdöhelyi and A. Szoke, Catal. Lett. 32 (1995) 43.

[9] L. Chen, L. Lin, Z. Xu, X. Li and T. Zhang, J. Catal. 157 (1995) 190.

[10] Y. Xu, Y. Shu, L. Wang, M. Xie and X. Guo, Catal. Lett. 35 (1995) 233.

[11] S.T. Wong, Y. Xu and X. Guo, Appl. Catal. A 136 (1996) 7.

[12] S.T. Wong, Y. Xu, L. Wang and M. Xie, Catal. Lett. 38 (1996) 39.

[13] N. Giordano, J.C.J. Bart, A. Vaghi, A. Castellan and G. Martinotti, J. Catal. 36 (1975) 81.

[14] N.K. Nag, J. Catal. 92 (1985) 432.

[15] C.V. Caceres, J.L.G. Fierro, A. Lopez Agudo, M.N. Blanco and H.J. Thomas, J. Catal. 95 (1985) 501.

[16] D.S. Zingg, L.E. Makovsky, R.E. Tischer, F.R. Brown and D.M. Hercules, J. Phys. Chem 84 (1980) 2898.

[17] G.D. Sun, T.Y. Yu, Q. Lu, Y. Jiao, L.G. Ren and F.S. Yan, J. Catal. (Chinese) 14 (1993) 62.

[18] D.L. Zhang, X.Q. Guo, X.L. Zeng and H.F. Xu, Chem. Anal. (Chinese) 5 (1977) 383.

[19] F.E. Massoth, Adv. Catal. 27 (1979) 265.

[20] J. Medema, C. van Stam, V.H.J. de Beer, A.J.A. Konings and D.C. Koningsberger, J. Catal. 53 (1978) 386.

[21] P. Arnoldy, J.A.M. van den Heijkant, G.D. de Bok and J.A. Moulijn, J. Catal. 92 (1985) 35.

[22] Z.B. Wei, Q. Xin, et al., Catal. Lett. 11 (1991) 365.

[23] A. Ezzamarty, E. Catherine, D. Cornet and J.F. Hemidy, in: *Zeolites: Facts, Figure, Future*, Studies in Surface Science and Catalysis, Vol. 49B, eds. P.A. Jacobs and R.A. van Santen (Elsevier, Amsterdam, 1989) p. 1025.

[24] J. Sanz, V. Fornes and A. Corma, J. Chem. Soc. Faraday Trans. I 84 (1988) 3113.

[25] K.C. Khulbe, R.S. Mann and C.D. Ajaka, Zeolites 13 (1993) 572.

[26] N.Y. Topsøe, K. Pedersen and E.G. Derouane, J. Catal. 70 (1981) 41.

[27] Y. Yang, X. Guo, M. Deng, L. Wang and Z.H. Fu, in: *Zeolites as Catalysts, Sorbents and Detergent Builders*, eds. H.G. Karge and J. Weitkamp (Elsevier, Amsterdam, 1989) p. 849.

[28] B.S. Kwak and W.M.H. Sachtler, J. Catal. 145 (1994) 456.

[29] L. Balkrishnan, B.S. Bao, S.G. Hedge, A.N. Kotasthane, S.B. Kulkarni and P. Ratnaswamy, J. Mol. Catal. 17 (1982) 261.

[30] S. Rajagopol, J.A. Marzari and R. Miranda, J. Catal. 151 (1995) 192.

[31] P. Ratnasamy, A.V. Ramaswamy, K. Banerjee, D.K. Sharma and N. Ray, J. Catal. 38 (1975) 19.

[32] G.J. Kramer, R.A. van Santen, C.A. Emeis and A.K. Nowak, Nature 363 (1993) 529.

[33] J. Sauer, Nature 363 (1993) 493.